Since January 2020 Elsevier has created a COVID-19 resource centre with free information in English and Mandarin on the novel coronavirus COVID-19. The COVID-19 resource centre is hosted on Elsevier Connect, the company's public news and information website.

Elsevier hereby grants permission to make all its COVID-19-related research that is available on the COVID-19 resource centre - including this research content - immediately available in PubMed Central and other publicly funded repositories, such as the WHO COVID database with rights for unrestricted research re-use and analyses in any form or by any means with acknowledgement of the original source. These permissions are granted for free by Elsevier for as long as the COVID-19 resource centre remains active.

VIROLOGY 221, 325–334 (1996)
ARTICLE NO. 0382

Syncytia Formation Induced by Coronavirus Infection Is Associated with Fragmentation and Rearrangement of the Golgi Apparatus

EHUD LAVI,*,[1] QIAN WANG,* SUSAN R. WEISS,† and NICHOLAS K. GONATAS*

*Department of Pathology and Laboratory Medicine, Division of Neuropathology, and †Department of Microbiology, University of Pennsylvania School of Medicine, Philadelphia, Pennsylvania 19104-6079

Received November 10, 1995; accepted May 8, 1996

Coronavirus mouse hepatitis virus (MHV) possesses a membrane glycoprotein (M) which is targeted to the Golgi apparatus (GA). We used immunocytochemistry with an organelle-specific antiserum to investigate the morphologic changes of the GA during infection of L2 murine fibroblasts with MHV-A59. Twenty-four hours after infection the GA was fragmented and translocated in the center of syncytia, while the microtubular network was also rearranged displaying radiating elements toward the center of syncytia. Two fusion-defective mutants, which contain an identical amino acid substitution in the cleavage signal sequence of the spike glycoprotein (S), induced fragmentation of the GA. However, the GA migrated only partially to the centers of syncytia during infection with these mutants. Revertant viruses, in which the above mutation was corrected, had fusion properties and GA staining similar to wtMHV-A59. Experiments with brefeldin A (BFA), which induces redistribution of the GA into the rough endoplasmic reticulum (RER), revealed that an intact GA for a period of 4–16 hr postinfection, is required for coronavirus replication and syncytia formation. Thus, during MHV infection, syncytia formation is associated with fragmentation of the GA, followed by a previously undescribed phenomenon of migration of the organelle into the centers of syncytia. The fragmentation of the GA, however, may occur without the formation of syncytia. Therefore, two distinct mechanisms may be responsible for the fragmentation of the GA and its subsequent migration to the center of syncytia. © 1996 Academic Press, Inc.

INTRODUCTION

Polypeptides synthesized in the rough endoplasmic reticulum (RER) and destined for plasma membranes, lysosomes, and secretion are transported through the Golgi apparatus for posttranslational modifications and targeting (Farquhar and Palade, 1981; Mellman and Simons, 1992; Rothman and Orci, 1992). The GA is a dynamic organelle which undergoes morphologic and functional modifications under physiologic and pathologic conditions. In mitotic Hela cells the GA disperses in early prophase and reaggregates in telophase (Robbins and Gonatas, 1964). During mitosis, the Golgi apparatus fragments into numerous small groups of vesicles which have been referred to as the mitotic form of the organelle (Lucocq *et al.,* 1987). In interphase cells treated with drugs which depolymerize microtubules, the GA fragments into small randomly distributed elements (Robbins and Gonatas, 1964; Turner and Tartakoff, 1989). In many cells the secretion blocker Brefeldin A (BFA) reversibly redistributes membranes and enzymes of the GA back into the RER, but does not inhibit endocytosis (Doms *et al.,* 1989; Lippincott-Schwartz *et al.,* 1989; Johnston *et al.,* 1994). Ricin, cholera toxin, and wheat germ agglutinin undergo endocytosis into the trans-Golgi-network (TGN), while shiga toxin is internalized into the GA and the RER (Sandvig *et al.,* 1991; Gonatas 1994). Pretreatment of cells with BFA protects them against the lethal effects of certain toxins, implying that the toxin's entry into TGN and the GA is necessary for translocation into their cytosolic targets (Yoshida *et al.,* 1991). In the human disease amyotrophic lateral sclerosis (ALS), the GA of spinal cord motor neurons is fragmented into numerous small elements which resemble the dispersion of the organelle induced by agents depolymerizing microtubules (Mourelatos *et al.,* 1990, 1993; Gonatas *et al.,* 1992). A similar fragmentation of the GA has been observed in motor neurons of transgenic mice expressing a mutant Cu,Zn superoxide dismutase (Mourelatos *et al.,* 1996).

Migration and rearrangements of the GA have been reported during syncytia formation and fusion of Vero cells infected with Sindbis virus (Ho *et al.,* 1990). Within 3–5 hr after infection, individual elements of the GA, which are associated initially with separate microtubule-organizing centers in perinuclear areas of fused cells, congregate in the center of syncytia and form an extended network of nondisrupted intact Golgi complexes (Ho *et al.,* 1990). In contrast to Sindbis infections, the Golgi apparatus is fragmented in cells infected with herpes simplex virus 1 (Campadelli *et al.,* 1993).

Infection of cultured cells with coronavirus MHV-A59

[1] To whom correspondence and reprint requests should be addressed. Fax: (215) 573-2059. E-mail: ehud_lavi.ap@path1a.med.upenn.edu.

0042-6822/96 $18.00
Copyright © 1996 by Academic Press, Inc.
All rights of reproduction in any form reserved.

is characterized by retention of the viral envelope glycoprotein M (previously known as E1) within the GA (Tooze *et al.,* 1988; Klumperman *et al.,* 1994; Krijnse-Locker *et al.,* 1994) and budding of virions from internal membranes (Holmes and Behnke, 1981; Tooze *et al.,* 1988). The close interaction between coronavirus particles with the GA provides an unusual opportunity to study morphologic and functional properties of the GA and various aspects of virus–cell interactions. In this study, we used organelle-specific antibodies, immunohistochemistry, and transmission electron microscopy to examine the fate of the GA during cell fusion and syncytia formation in mouse L-2 cells infected with MHV-A59 and fusion defective mutants. Fragmentation of the GA into small immunostained elements occurred prior to their migration into the centers of syncytia. Experiments with BFA revealed that the period of 4–16 hr postinfection is critical for coronavirus replication and syncytia formation. The results of studies with fusion defective mutants suggest that different mechanisms are responsible for the initial fragmentation of the GA and its subsequent migration to the centers of syncytia.

MATERIALS AND METHODS

Cell cultures

L-2 cells (murine fibroblasts), originally obtained from American Type Culture Collection (ATCC; Rockville, MD), were used to maintain viral growth cultures, preparation of viral stocks, and viral plaque assays. In some experiments 17Cl-1 murine fibroblasts were used. The cultures were maintained in DMEM/heat-inactivated 10% fetal bovine serum/1% Pen/Strep/4500 mg/liter D-glucose/L-glutamine.

Viruses and infections

Three times plaque purified MHV-A59 stock virus was used as previously described (Lavi and Weiss, 1989). Fusion defective mutants and revertants were prepared as previously described (Gombold *et al.,* 1993; Hingley *et al.,* 1994). Infections of cultures were done by incubation of virus with cells for 1 hr at a multiplicity of infection (m.o.i.) of 1, followed by washing of cells with fresh medium three times.

Organelle specific antibodies

MG-160 is a conserved sialoglycoprotein of the medial cisternae of the GA. The preparations of the anti-MG-160 monoclonal antibody (10A8), and the immunoaffinity purified anti-MG-160 polyclonal antibodies, were described in previous publications (Gonatas *et al.,* 1989; Croul *et al.,* 1988, 1990). The preparation of the monoclonal antibody 2H1, a RER marker of a 60- to 65-kDa protein, has been previously described (Chen *et al.,* 1991). The primary structure of MG-160 revealed significant homology with a chicken fibroblast growth factor receptor and a ligand to E-selectin (Gonatas *et al.,* 1995; Steegmaier *et al.,* 1995). In chicken, MG-160 appears early in development and the gene coding the protein, named GLG1, has been assigned to chromosome 16 (Stieber *et al.,* 1995; Mourelatos *et al.,* 1995).

Immunohistochemistry

Cells, grown on poly-D-lysine-treated coverslips, were fixed with 2% paraformaldehyde for 20 min at room temperature, washed three times in PBS, then incubated for 30 min in 0.05% Saponin/10% goat serum (GS) in PBS and washed three times in 10% GS in PBS. Cells were then incubated with primary antibody (1:1000 dilution in PBS of immunoaffinity-purified rabbit anti-MG-160 antibodies or with a supernatant from the anti MG-160 hybridoma (10A8) overnight at room temperature. Cultures were then washed, incubated with a biotinylated goat anti-rabbit IgG antibody, incubated with the avidin–biotin complex (ABC), and stained with diaminobenzidine tetrahydrochloride (DAB) (5 mg DAB/10 ml Tris-saline containing 10 m*M* Imidazole and 0.03% H_2O_2), according to standard methods (Graham and Karnovsky, 1966; Guesdon *et al.,* 1979).

Electron microscopy

Cells grown on Thermanox plastic (EM Sciences, Fort Washington, PA), were fixed overnight at 4° with 2.5% glutaraldehyde + 1% paraformaldehyde in 0.1% cacodylate buffer, pH 7.4, + 0.002% $CaCl_2$. Subsequently cultures were postfixed in 1% osmium tetroxide + 1.5% potassium ferrocyanide, dehydrated in ethanol, and embedded in Araldite. Sections (8–10 nm thick) were stained with lead and uranyl salts and viewed in a transmission electron microscope (JEOL 100 CX) at 80 kv (Karnovsky, 1971; Stieber *et al.,* 1987).

Viral infectivity assay

Viral titers were determined by duplicate plaque assays of several 10-fold dilution of samples in L-2 cell grown in six-well plates (Lavi *et al.,* 1984).

Brefeldin A (BFA) treatment

BFA (Sigma) stock solution (5 mg/ml in ethanol) was diluted in PBS and applied to cultures at a concentration of 5 μg/ml for periods of 1 hr or longer, as specifically indicated in the text (Fig. 3). In control experiments cultures were incubated for the same time periods with the same dilution of ethanol used to dissolve BFA.

RESULTS

Changes of the GA during MHV infection and formation of syncytia

Morphological changes of the GA during coronavirus infection of L2 cells (4, 8, 16, 24, and 48 hr) were examined by immunocytochemistry using organelle-specific antibodies (Croul *et al.,* 1988, 1990; Gonatas *et al.,* 1989). Typical infection of L2 cells with MHV-A59 caused syncytia formation of the entire monolayer within 24 hr and complete cytolysis within 48 hr. At 16 hr postinfection, cell borders were indistinct and the nuclei were aggregated; by 24 hr postinfection, the syncytia acquired their typical morphology consisting of a ring of nuclei surrounding a cytoplasmic center devoid of nuclei. Between 24 and 48 hr postinfection, cells underwent pyknosis, karyorhexis, and then died and detached from the culture dish.

The immunostained GA of uninfected cells formed contiguous coarsely granular focal or ring-like perinuclear profiles (Figs. 1A and 1D). Following infection of L2 cells with MHV-A59, the coarsely granular stain of the GA became fine and smaller individual elements of the GA were discernible. At 16 hr postinfection, the majority of the syncytia consisted of clustered nuclei within a cytoplasmic mass, lacking distinguishable cell borders; in those syncytia, the immunostained GA appeared as strands of finely granular elements forming a honeycomb-like network with interspersed nuclei (Figs. 1B and 1E). However, before full syncytia formation, in cells surrounding the forming syncytia the distribution of the GA was perinuclear, similar to that of controls but with finer granular GA elements (compare Figs. 1E and 1D). This phenomenon probably represented an early stage of fragmentation and rearrangement of the GA. At 24 hr postinfection, the process of fragmentation of the GA and its relocation in the centers of syncytia, as well as the rearrangement of the nuclei in a ring formation within the syncytia, was complete (Figs. 1C and 1F). The honeycomb morphology due to the interspersed nuclei was replaced by a typical central aggregate of finely granular or fragmented GA, surrounded by a rim of nuclei (compare Figs. 1F with 1E). Furthermore, the nuclei in the syncytium were not surrounded by any residual GA. Thus, in the fully developed syncytium, all elements of the fragmented GA had moved into the center, while the more peripherally arranged nuclei formed a ring devoid of adjacent elements of the GA (Fig. 1F). Staining of syncytia with rabbit anti-MHV polyclonal antibodies revealed an abundance of viral proteins in the center of syncytia (not shown).

In order to determine whether the fragmentation and rearrangement of the GA was cell-type dependent, another cell line, 17Cl-1 murine fibroblasts, was infected with MHV-A59. This cell line supports both cell fusion and cyncytia formation when infected with MHV-A59. Following infection, cells were fixed and examined by immunohistochemistry with identical methods used for L2 cells. The changes in the GA observed in these cells were identical to those seen in L2-infected cells.

Changes of the GA following infection of L2 cells with fusion-defective mutants and a fusion-negative strain of MHV

To investigate whether the fragmentation of the GA is dependent on cell fusion, we examined the organelle in L2 cells infected with two fusion defective mutants of MHV-A59. The C12 and B11 mutants, used in these experiments, were isolated from primary cultures of glial cells infected with MHV-A59. These mutants are fusion-delayed and defective but not fusion-negative and produce reduced number of syncytia formations. Thus at any given time point postinfection with the mutant viruses, only a small percentage of L2 cells form syncytia, as compared to cells infected with MHV-A59 (Gombold *et al.,* 1993). These fusion-defective mutants have a histidine to aspartic acid mutation (H716D) within the cleavage signal of the spike (S) glycoprotein. Cleavage of S is necessary for efficient cell fusion during MHV-A59 infection (Gombold *et al.,* 1993). Infection with these mutant viruses does not affect the efficiency of viral replication or titers of infectious virus (Gombold *et al.,* 1993). Immunostaining of the GA in L2 cultures infected with the fusion defective mutants B11 and C12 showed fragmentation of the GA similar to that found in cells infected with MHV-A59. However, the translocation and rearrangement of the GA during infection with these two mutant viruses was distinctly different from the changes of the organelle seen during infections with the wild-type MHV-A59. Specifically, cells infected with either B11 or C12 mutants displayed both central and peripheral aggregates of finely granular GA (Figs. 1H and 1I). The granular stain of the GA at the periphery of syncytia, and specifically around the peripherally located nuclei, was observed only in cultures infected with these two mutant viruses. This pattern of GA distribution was not seen in any of the stages of MHV-A59 viral replication (compare Figs. 1I and 1F). In order to rule out the possibility that the fusion-defective variants showed only delay in translocation of the GA into the center of cyncytia, immunocytochemical analysis was performed at 36 and 48 hr after viral infection. These experiments showed that the typical complete central translocation of the GA, similar to that seen in A59-infected cultures, never occurred in cultures infected with the two fusion defective mutants, even prior to or at the stage of complete cell death.

To further explore the link between fragmentation of the GA and fusion we then infected L2 cells with MHV-2, a fusion-negative strain of MHV. L2 cells are suscepti-

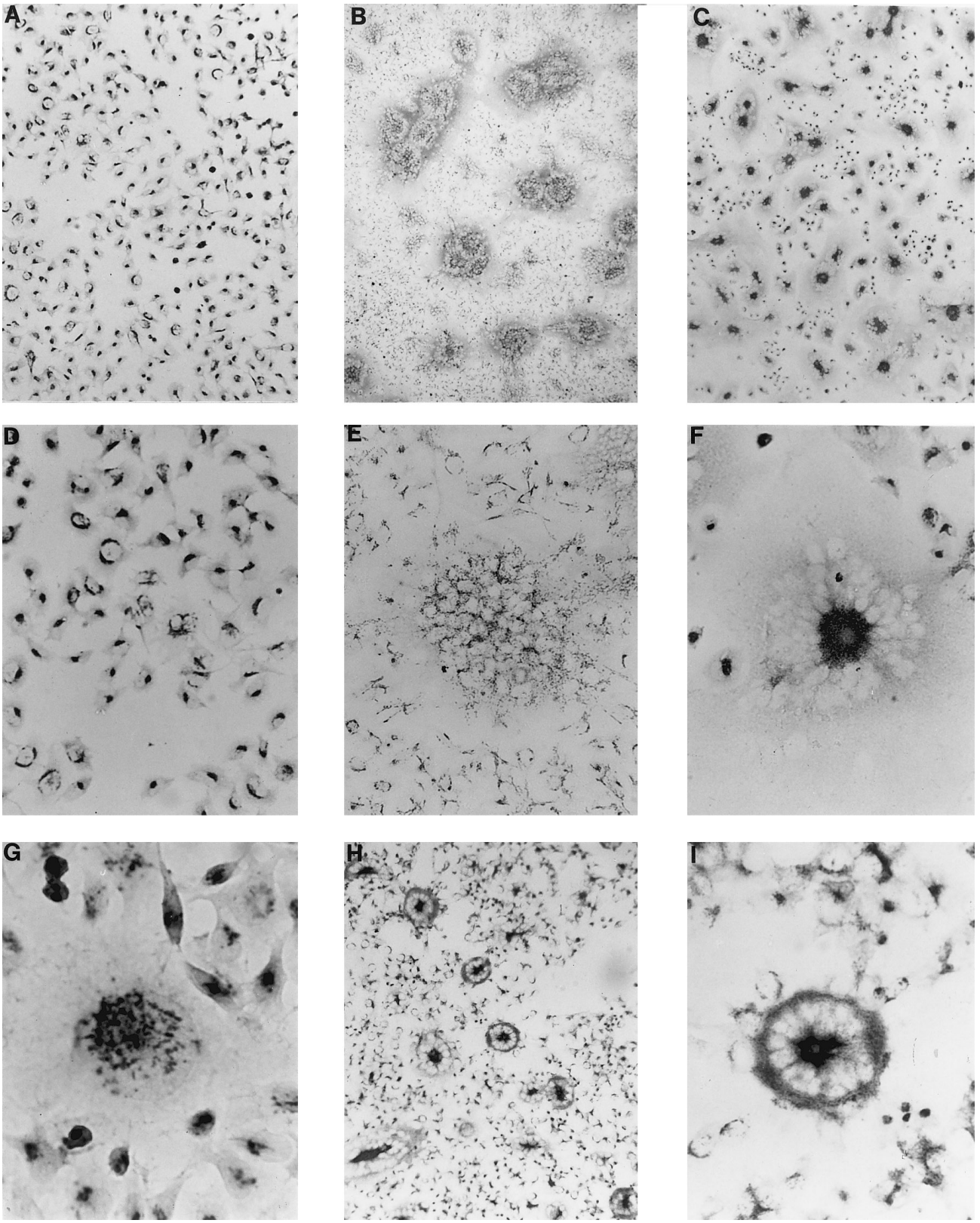

FIG. 1. Immunohistochemistry on uninfected L-2 cells (fibroblasts) with an antibody against MG-160, a Golgi apparatus (GA)-specific protein showing coarse granular focal juxtanuclear or perinuclear staining of the GA in each cell. Low magnification of ×100 (A) and higher magnification ×200 (D). Immunohistochemistry on L-2 cells 16 hr after infection with MHV-A59 (B, E). Staining with antibodies against MG-160 shows fragmentation and a network or honeycomb distribution of the GA within the syncytia formed in infected fibroblasts. Note normal GA of cells at the periphery and not participating in the formation of the syncytia. Low magnification of ×100 (B) and higher magnification of ×200 (E). Immunohistochemistry on L-

ble to cytopathic infection with this strain and are completely destroyed after 48 hr with titers similar to MHV-A59. However, there was no cell fusion or syncytia formation in these cultures. Infection with MHV-2 produced dispersion and fragmentation of the GA in individual cells, some of which appeared to be balooned after 24 hr (Fig. 1G). These observations are consistent with the conclusion that the fragmentation of the GA during infection with MHV is independent of cell fusion. However, the translocation of the GA in the center of the syncytia is probably linked to cell fusion since fusion-defective mutants were also defective in their ability to induce translocation of the GA to the center of the syncytia.

Ultrastructural changes of the GA in MHV-infected cells

To further investigate the morphologic aspects of the fragmented GA in syncytia of L2 cells infected with MHV-A59, an electron microscopic examination was performed in cells 24 hr after infection and at a multiplicity of infection (m.o.i.) of 1 plaque forming unit per cell. Areas of syncytia with a typical peripheral rim of nuclei were selected from semithin (0.5–1 μm) sections. In uninfected cells the GA was seen in a perinuclear location and consisted of several groups of stacked cisternae surrounded by numerous coated and uncoated vesicles (Fig. 2B). In contrast to this typical morphology of the GA, in infected cells the stacks of the cisternae were markedly diminished in size and were replaced by numerous tubulovesicular structures, some of which containing virus particles (Fig. 2A). Furthermore, in infected cells the region containing remnants of GA cisternae and the abundant tubulovesicular structures was rich in transversing microtubules (Fig. 2A).

The distribution of the RER is not affected by MHV-A59 infection

The distribution of the RER in MHV-A59-infected and control L2 cells was investigated by immunocytochemistry with the organelle-specific monoclonal antibody 2H1 (Chen *et al.,* 1991). There was no detectable difference between the infected and uninfected cells in the immunostaining of the RER. In both cases the fine granular staining of the RER was evenly distributed within the entire cytoplasm including the centers of syncytia (not shown).

The network of microtubules is rearranged during MHV-A59 infection

Since the GA is associated with microtubules of interphase cells (Robbins and Gonatas, 1964; Turner and Tartakoff, 1989), we investigated whether microtubules are affected during coronavirus infection. Specifically, we investigated whether the fragmentation of the GA within the centers of the syncytia is associated with a similar change of the microtubules. The immunocytochemical staining of the GA at 4, 8, 16, 24, and 48 hr after MHV-A59 infection was compared with the immunostaining of microtubules with antibodies against alpha and beta tubulin. While the GA appeared fragmented early during infection and syncytia formation, fragmentation and disintegration of microtubules occurred late (48 hr), when cells die. The kinetics of the microtubule changes after infection with MHV-A59 was depicted by immunofluorescence on L-2 cells after infection with MHV-A59 (m.o.i. = 1 PFU/cell) and after staining with anti-tubulin antibodies and FITC-conjugated secondary antibodies (Fig. 3). In uninfected cells and at 4 hr postinfection the microtubules were distributed throughout the entire cytoplasm of the individual cells. At 16 hr postinfection the syncytia were beginning to form and the microtubules were still distributed within the entire cytoplasm. At 24 hr postinfection, when the GA was fragmented and translocated to the centers of syncytia, the microtubules were rearranged in a characteristic pattern (Fig. 3). Specifically, at the periphery of the syncytia, an intense stain for tubulins suggested that the nuclei were surrounded by a rich network of microtubules. At the intermediate zone, between the periphery and the center of syncytia, the microtubules formed a radiating network. At the center of the syncytia, the immunostain for alpha and beta tubulin was less intense and amorphous (Fig. 3). These changes suggest that during coronavirus infection the microtubules undergo rearrangement and perhaps provide guidance for the translocation of the fragmented elements of the GA into the center of the syncytia.

The effect of Brefeldin A on coronavirus infection

Since coronavirus infection is associated with the processing of viral proteins through the GA, including retention and budding of the viral glycoprotein M

2 cells 24 hr after infection with MHV-A59 (C, F). Staining with antibodies against MG-160 shows central location of the fused and fragmented GA within the syncytia formation of infected fibroblasts. Low magnification of ×100 (C) and higher magnification of ×200 (F). Immunohistochemistry on L-2 cells 24 hr after infection with B11, a fusion-defective variant of MHV-A59 (H, I). Staining with a GA-specific antibody shows fragmentation but incomplete translocation of the GA into the center of the syncytia formation of infected cells. Low magnification of ×100 (H) and high magnification of ×200 (I). Immunohistochemistry on L-2 cells 24 hr after infection with MHV-2 and staining with anti MG-160 antibodies (G). Note fragmentation of the GA and dispersion of the staining throughout the cytoplasm of a balooned cell without syncytia formation ×400. All the pictures were stained with DAB without counter staining.

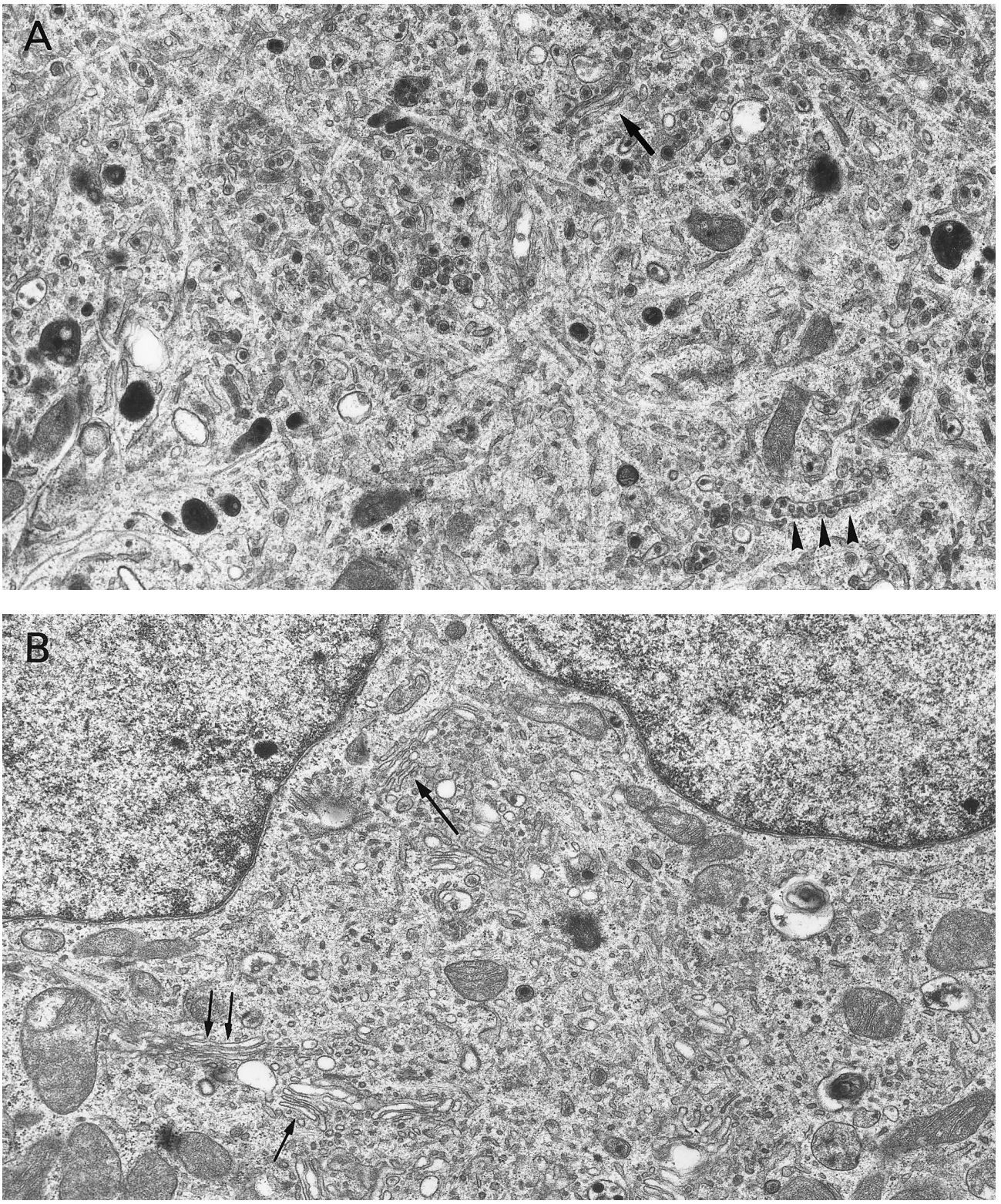

FIG. 2. (A) Electronmicrograph of syncytia formation in MHV-A59-infected L-2 cells. The center of the syncytia contains numerous fragmented Golgi apparatus structures (arrow) and viral particles (arrowheads). (B) Electronmicrograph of uninfected L-2 cells. Note normal Golgi apparatus (arrows).

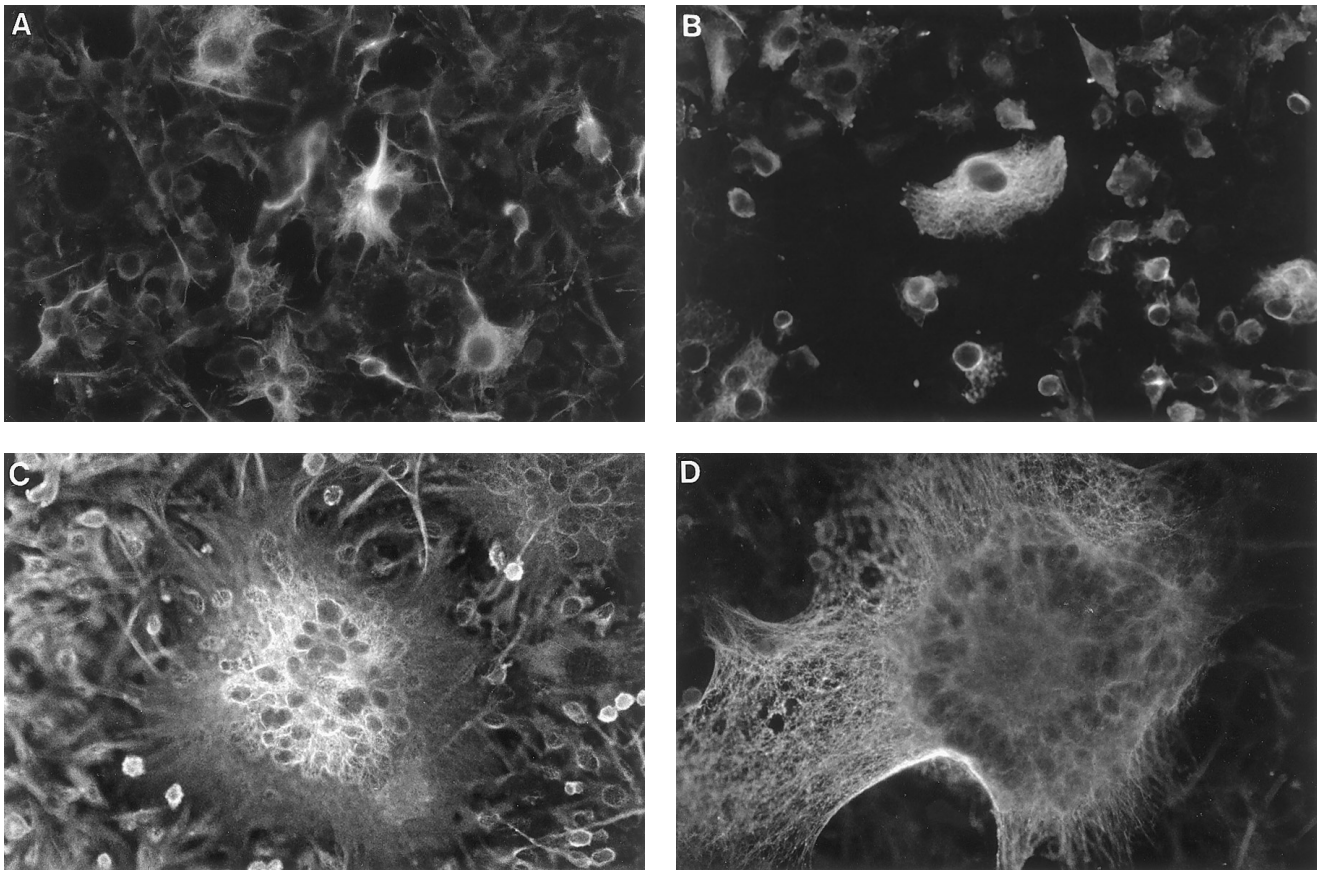

FIG. 3. Cytoskeleton changes after infection with MHV-A59 are depicted here by immunofluorescence study on L-2 cells after infection with MHV-A59 (m.o.i. = 1 PFU/cell) and staining with anti-tubulin antibodies and FITC-conjugated secondary antibodies. This cytoskeleton protein is distributed throughout the entire cytoplasm of the individual cells in uninfected (3A) and at 4-hr-infected cells (3B). At 16 hr postinfection the syncytia formation is beginning to form and the tubulin is distributed within the center of the syncytia (3C). At 24 hr postinfection there is more pronounced staining at the periphery of the syncytia (3D).

within the organelle, we investigated the effect of BFA on the morphology and kinetics of coronavirus infection. As summarized in Fig. 4, BFA was introduced at various time points during infection of L2 cell with MHV-A59. In uninfected L2 cells incubated for 1 hr with 5 μg/ml of BFA, immunostaining with anti-MG-160 showed a diffuse cytoplasmic pattern consistent with the known redistribution of MG-160 and other Golgi markers within the RER (Doms *et al.,* 1989; Lippincott-Schwartz *et al.,* 1989; Johnston *et al.,* 1994). Following 1 hr of BFA treatment at the beginning of infection cells had diffuse staining of the GA when observed 8 hr postinfection as did uninfected cells following a similar treatment with BFA. However, at 16 hr postinfection (and 1 hr of treatment with BFA at the beginning of infection) there was incomplete recovery from the BFA effect. In uninfected cells treated in a similar fashion with BFA, the recovery was complete. Therefore, when cells were infected with MHV-A59 prior to or at the same time of treatment with BFA, the effect of the drug on the GA was not abolished 16 or 24 hr later. Uninfected cells, however, had completely recovered from the BFA effect 16–24 hr later. These findings suggest that virus infection accentuates and prolongs the BFA effect (Fig. 4).

When cells were treated continuously with BFA during infection there was dispersion of the GA, lack of syncytia formation, and no detectable viral titers (Fig. 4). If BFA treatment began at 4 or 6 hr after viral inoculation, the effect of this treatment on infection was similar to the effect observed after continuous BFA treatment (i.e., reduced syncytia formation and no viral titers). However, when the BFA treatment began 12 hr or more after viral inoculation, there were relatively minimal effects on syncytia formation, and viral titers were 1–2 logs lower as compared to viral titers without BFA treatment (which usually fluctuate about 1–1.5 logs in various experiments).

When BFA was introduced 20 min or an hour before inoculation and continued through the entire infection or 1, 3, or 5 hr after inoculation, there was no significant effect on the ability of the virus to form syncytia 24 hr

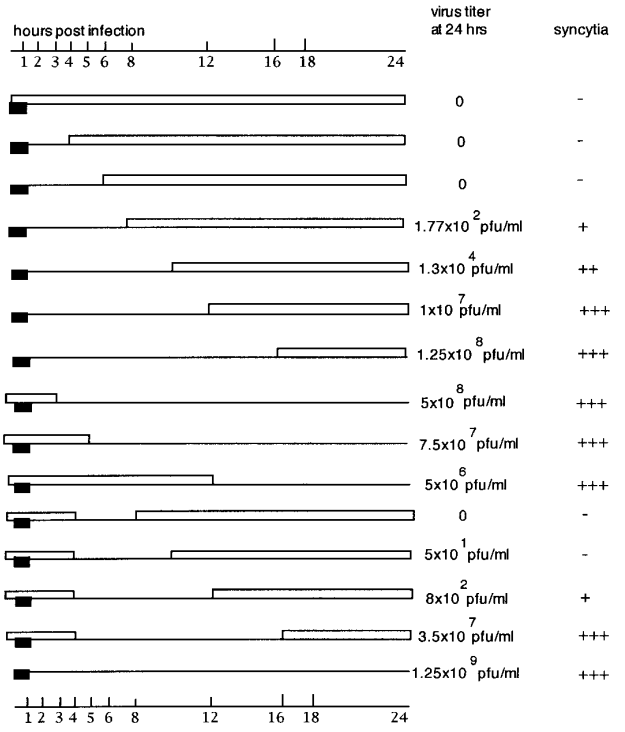

FIG. 4. The effect of BFA on infection of L-2 cells with MHV-A59. Cultures were incubated with virus (■) for 1 hr and exposed to BFA (▭) for various periods. At the end of 24-hr incubation the cultured cells were stained for MG-160 by immuohistochemistry and the supernatants were titered for virus by plaque assay. Titers labeled 0 indicate levels below 50 PFU/ml, which is the lowest level of detection in this assay.

postinfection and viral titers at that time were only 1–1.5 logs lower than without treatment. Thus BFA did not block the endocytosis and the initial processing of the virus into cells. BFA reduced viral replication only by 1–2 logs when introduced at 12–24 or 16–24 hr after infection. The results of the exposure to BFA at the beginning of infection for 4 hr and for various periods at the end of infection (Fig. 4) indicated that the BFA effect on the GA during 4–16 hr postinoculation was associated with reduced viral replication. If BFA was introduced after or before this stage (4–16 hr), there was no effect on viral replication, assembly, and maturation. These results suggest that the interval of 4–16 hr postinfection is the most significant period requiring an intact GA for viral replication and syncytia formation. This conclusion is based on infection at an m.o.i. of 1 PFU/cell which may be an asynchronous infection. In a more synchronous infection the period of BFA effect may terminate earlier than 16 hr postinfection.

DISCUSSION

The GA plays an important role in the life cycle of many viruses such as vaccinia, CMV, bunyaviruses, and coronaviruses. Vaccinia virus DNA becomes enwrapped by cisternae derived from the intermediate compartment between the ER and the Golgi stacks, thus acquiring two membranes in one step (Sodeik *et al.,* 1993, 1995). The second wrapping cisternae in vaccinia virus assembly is derived from the trans Golgi network (Schmelz *et al.,* 1994). In CMV, ultrastructural as well as biochemical studies suggested that short-term exposure of infected cultures to BFA during the late infectious cycle primarily prevented Golgi-dependent processes, e.g., envelopment of naked cytoplasmic nucleocapsids in the trans-Golgi network (TGN) and normal processing of glycoprotein B (Eggers *et al.,* 1992). In Uukuniemi virus, a member of the bunyaviridae, immunofluorescent staining indicated that G1 glycoprotein expressed alone localized to the GA. G2 expressed alone was associated with the RER (Melin *et al.,* 1995). Coronavirus MHV M glycoprotein (previously known as E1) is targeted to the GA and contains a retention signal for the GA (Machamer *et al.,* 1990; Swift and Machamer, 1991; Armstrong and Patel, 1991).

Previous reports have shown that the GA undergoes rearrangement (Ho *et al.,* 1990) and fragmentation (Campadelli *et al.,* 1993) in viral infections. The data presented here detail the changes in the morphology of the GA in cells infected by a virus which induces the formation of syncytia. In coronavirus infection, the virus displays complex and close interactions with the GA. In coronavirus-induced syncytia formation there is a unique translocation and aggregation of the GA into the center of the syncytia which is not accompanied by similar changes of the RER and cytoskeleton (Fig. 1F). The observed fragmentation of the GA is not related to the formation of syncytia as demonstrated by the experiments using a fusion-negative strain of MHV and fusion-defective mutants in which fragmentation of the GA also occurs. Fragmentation and translocation of the GA may be important in the life cycle of coronavirus replication. Further studies are necessary to determine whether there are viruses that replicate within cells without causing alteration of GA morphology.

Central translocation and aggregation of the GA may be unique to coronaviruses as it was not associated with other fusion and syncytia forming viruses such as Sindbis virus infection (Ho *et al.,* 1990) or herpes simplex virus infection (Campadelli *et al.,* 1993). Since the aggregation of the fragmented GA in the centers of syncytia has not been previously reported, we investigated the GA in cells infected with LaCrosse bunyavirus, which is known to induce the formation of syncytia (Gonzalez-Scarano *et al.,* 1984). Immunostaining of the GA in BHK cells infected with LaCrosse virus for 24 hr showed network formation and fragmentation of the GA, without the aggregation of the GA into centralized zones and without the formation of amorphous centers of syncytia which is characteristic of MHV infection (unpublished observations). Thus the translocation of the GA to the center of the syncytia may

be related to a unique interaction between coronavirus proteins with the membranes of the GA.

Since mutant viruses that are defective in their ability to cause efficient fusion are also inefficient in translocating the GA to the center of the syncytia, the translocation of the GA appears to be linked to the ability of the virus to cause fusion. Although the fusion property has been associated with the S gene and the site encoding cleavage of the S protein (Gombold *et al.,* 1993), other reports showed that cleavage of the S gene in coronaviruses is not an absolute requirement for fusion (Stauber *et al.,* 1993; Taguchi *et al.,* 1993). However, fragmentation of the GA was unaffected by the lack of fusion in MHV-2 or by the mutation that caused inefficient fusion of the virus in fusion-defective mutants. This suggests that determinants responsible for the fragmentation of the GA are unrelated to fusion determinants or to the mutation of the cleavage site on the S gene. Additional studies are necessary to precisely identify the domain of the viral genome associated with fragmentation of the GA.

The close association between coronavirus replication cycle and an intact GA is further emphasized in the experiments with the secretion blocker BFA. BFA treatment, especially for long intervals, has an adverse effect on viral replication and maturation and viral replication delays recovery of the GA from BFA effect. This reciprocal interaction between viral replication and the GA may be useful in future studies of aspects of both viral replication and the biology of the GA.

ACKNOWLEDGMENTS

The authors thank Anna Stieber for excellent technical assistance with the EM work, Jackie Gonatas for the anti-MG-160 antibodies, Yojun Chen for the anti-RER antibodies, Dr. Francisco Gonzalez-Scarano for the help with experiments using LaCrosse virus, and Dr. Mikhail Rozanov for critical review of the manuscript. This study was supported in part by National Multiple Sclerosis Society Grants PP-0284, RG-2615A1/2 (E.L.), a grant from the University of Pennsylvania Research Foundation (E.L.), PHS Grants NS-21954 (S.R.W.), and Javits Neuroscience Award NS-05572 (N.K.G.). Parts of this work were presented at the Sixth International Symposium on Corona and Related Viruses in Quebec City, Canada, September 1994.

REFERENCES

Armstrong, J., and Patel, S. (1991). The Golgi sorting domain of coronavirus E1 protein. *J. Cell Sci.* 98, 567–575.

Campadelli, G., Brandimarti, R., Di Lazzaro, C., Ward, P. L., Roizman, B., and Ttorrisi, M. R. (1993). Fragmentation and dispersal of Golgi proteins and redistribution of glycoproteins and glycolipids processed through the Golgi apparatus after infection with herpes simplex virus 1. *Proc. Natl. Acad. Sci. USA* 90, 2798–2802.

Chen, Y., Hickey, W. F., Mezitis, S. G. E., Stieber, A., Lavi, E., Gonatas, J. O., and Gonatas, N. K. (1991). Monoclonal antibody 2H1 detects a 60-65 kD membrane polypeptide of the rough endoplasmic reticulum of neurons and stains selectively cells of several rat tissues. *J. Histochem. Cytochem.* 39, 635–643.

Croul, S. E., Mezitis, S. G. E., and Gonatas, N. K. (1988). An anti-organelle antibody in pathology. The chromatolytic reaction studied with a monoclonal antibody against the Golgi apparatus. *Am. J. Pathol.* 133, 355–362.

Croul, S. E., Mezitis, S. G. E., Stieber, A., Chen, Y., Gonatas, J. O., Goud, B., and Gonatas, N. K. (1990). Immunohistochemical visualization of the Golgi apparatus in several species, including human, and tissue with antiserum against MG-160, a sialoglycoprotein of rat Golgi apparatus. *J. Histochem. Cytochem.* 38, 957–963.

Doms, R. W., Russ, G., and Yewdell, J. W. (1989). Brefeldin A redistributes resident and itinerant Golgi proteins to the endoplasmic reticulum. *J. Cell Biol.* 109, 61–72.

Eggers, M., Bogner, E., Agricola, B., Kern, H. F., and Radsak, K. (1992). Inhibition of human cytomegalovirus maturation by brefeldin A. *J. Gen. Virol.* 73, 2679–2692.

Farquhar, M. G., and Palade, G. E. (1981). The Golgi apparatus (complex)-(1951–1981) from artifact to center stage. *J. Cell. Biol.* 91, 77S–103S.

Gombold, J. L., Hingley, S. T., and Weiss, S. R. (1993). Fusion-defective mutants of mouse hepatitis virus A59 contain a mutation in the spike protein cleavage signal. *J. Virol.* 67, 4504–4512.

Gonatas, J. O., Mezitis, S. G. E., Stieber, A., Fleischer, B., and Gonatas, N. K. (1989). MG-160, a novel sialoglycoprotein of the medial cisternae of the Golgi apparatus. *J. Biol. Chem.* 264, 646–653.

Gonatas, J. O., Mourelatos, Z., Stieber, A., Lane, W. S., Brosius, J., and Gonatas, N. K. (1995). MG-160, a membrane sialoglycoprotein of the medial cisternae of the rat Golgi apparatus, binds basic fibroblast growth factor and exhibits a high level of sequence identity to a chicken fibroblast growth factor receptor. *J. Cell. Sci.* 108, 457–467.

Gonatas, N. K. (1994). Contributions to the physiology and pathology of the Golgi apparatus. *Am. J. Pathol.* 145, 751–761.

Gonatas, N. K., Stieber, A., Mourelatos, Z., Chen, Y., Gonatas, J. O., Appel, S. H., Hays, A. P., Hickey, W. F., and Hauw, J. J. (1992). Fragmentation of the Golgi apparatus of motor neurons in amyotrophic lateral sclerosis. *Am. J. Pathol.* 140, 1–7.

Gonzalez-Scarano, F., Pobjecky, N., and Nathanson, N. (1984). LaCross Bunyavirus can mediate pH-dependent fusion from without. *Virology* 132, 222–225.

Graham, C. R., and Karnovsky, M. J. (1966). The early stages of absorption of injected horseradish peroxidase in the proximal tubules of mouse kidney: Ultrastructural cytochemistry by a new technique. *J. Histochem. Cytochem.* 14, 291–302.

Guesdon, J.-L., Ternynck, T., and Avrameas, S. (1979). The use of avidin-biotin interaction in immunoenzymatic techniques. *J. Histochem. Cytochem.* 27, 1131–1139.

Hingley, S. T., Gombold, J. L., Lavi, E., and Weiss, S. R. (1994). MHV-A59 fusion mutants are attenuated and display altered hepatotropism. *Virology* 200, 1–10.

Ho, W. C., Storrie, B., Pepperkok, R., Ansorge, W., Karecla, P., and Kreis, T. E. (1990). Movement of interphase Golgi apparatus in fused mammalian cells and its relationship to cytoskeletal elements and rearrangement of nuclei. *Eur. J. Cell. Biol.* 52, 315–327.

Holmes, K. V., and Behnke, J. N. (1981). Evolution of a coronavirus during persistent infection in vitro. *Adv. Exp. Med. Biol.* 142, 287–299.

Johnston, P. A., Stieber, A., and Gonatas, N. K. (1994). A hypothesis on the traffic of MG-160, a medial Golgi sialoglycoprotein, from the trans Golgi Network to the Golgi cisternae. *J. Cell. Sci.* 107, 527–533.

Karnovsky, M. J. (1971). Use of ferrocyanide-reduced osmium tetroxide in electron microscopy. *Eleventh annual meeting of the American Society for Cell Biology.* Abstract 284, 146.

Klumperman, J., Locker, J. K., Meijer, A., Horzinek, M. C., Geuze, H. J., and Rottier, P. J. (1994). Coronavirus M proteins accumulate in the Golgi complex beyond the site of virion budding. *J. Virol.* 68, 6523–6534.

Krijnse-Locker, J., Ericsson, M., Rottier, P. J., and Griffiths, G. (1994). Characterization of the budding compartment of mouse hepatitis

virus: evidence that transport from the RER to the Golgi complex requires only one vesicular transport step. *J. Cell Biol.* 124, 55–70.

Lavi, E., Gilden, D. H., Wroblewska, Z., Rorke, L. B., and Weiss, S. R. (1984). Experimental demyelination produced by the A59 strain of mouse hepatitis virus. *Neurology* 34, 597–603.

Lavi, E., and Weiss, S. R. (1989). Coronaviruses. *In* "Clinical and Molecular Aspects of Neurotropic Viral Infections" pp. 101–139. Kluwer Academic Publishers, Boston.

Lippincott-Schwartz, J., Yuan, L. C., Bonifacino, J. S., and Klausner, R. D. (1989). Rapid redistribution of Golgi proteins into the ER in cells treated with Brefeldin A: evidence for membrane cycling from Golgi to ER. *Cell* 56, 801–813.

Lucocq, J. M., Pryde, J. G., Berger, E. G., and Warren, G. (1987). A mitotic form of the Golgi apparatus in HeLa cells. *J. Cell. Biol.* 104, 865–874.

Machamer, C. E., Mentone, S. A., Rose, J. K., and Farquhar, M. G. (1990). The E1 glycoprotein of an avian coronavirus is targeted to the cis Golgi complex. *Proc. Natl. Acad. Sci. USA* 87, 6944–6948.

Melin, L., Persson, R., Andersson, A., Bergstrom, A., Ronnholm, R., and Pettersson, R. F. (1995). The membrane glycoprotein G1 of Uukuniemi virus contains a signal for localization to the Golgi complex. *Virus Res.* 36, 49–66.

Mellman, I., and Simons, K. (1992). The Golgi complex: In vitro veritas? *Cell* 68, 829–840.

Mourelatos, Z., Adler, H., Hirano, A., Donnenfeld, H., Gonatas, J. O., and Gonatas, N. K. (1990). Fragmentation of the Golgi apparatus of motor neurons in amyotrophic lateral sclerosis revealed by organelle-specific antibodies. *Proc. Natl. Acad. Sci. USA* 87, 4393–4395.

Mourelatos, Z., Gonatas, J. O., Nycum, L. M., Gonatas, N. K., and Biegel, J. A. (1995). Assignment of the GLG1 gene for MG-160, a fibroblast growth factor and E-Selectin binding membrane sialoglycoprotein of the Golgi apparatus, to chromosome 16q22-q23 by fluorescence in situ hybridization. *Genomics* 28, 354–355.

Mourelatos, Z., Gonatas, N. K., Stieber, A., Gurney, M. E., and Dal Canto, M. C. (1996). The Golgi apparatus of spinal cord motor neurons in transgenic mice expressing mutant Cu,Zn superoxide dismutase (SOD) becomes fragmented in early, preclinical stages of the disease. *Proc. Natl. Acad. Sci. USA,* in press.

Mourelatos, Z., Yachnis, A., Rorke, L., Mikol, J., and Gonatas, N. K. (1993). The Golgi apparatus of motor neurons in amyotrophic lateral sclerosis. *Ann. Neurol.* 33, 608–615.

Robbins, E., and Gonatas, N. K. (1964). Histochemical and ultrastructural studies of HeLa cells during the mitotic cycle. *J. Histochem. Cytochem.* 12, 704–711.

Robbins, E., and Gonatas, N. K. (1964). The ultrastructure of a mammalian cell during the mitotic cycle. *J. Cell. Biol.* 21, 429–463.

Rothman, J. E., and Orci, L. (1992). Molecular dissection of the secretory pathway. *Nature* 355, 409–415.

Sandvig, K., Prydz, K., Hansen, S. H., and Van Deurs, B. (1991). Ricin transport in brefeldin A-treated cells: correlation between Golgi structure and toxic effect. *J. Cell Biol.* 115, 971–981.

Schmelz, M., Sodeik, B., Ericsson, M., Wolffe, E. J., Shida, H., Hiller, G., and Griffiths, G. (1994). Assembly of vaccinia virus: The second wrapping cisterna is derived from the trans Golgi network. *J. Virol.* 68, 130–147.

Sodeik, B., Cudmore, S., Ericsson, M., Esteban, M., Niles, E. G., and Griffiths, G. (1995). Assembly of vaccinia virus: Incorporation of p14 and p32 into the membrane of the intracellular mature virus. *J. Virol.* 69, 3560–3574.

Sodeik, B., Doms, R. W., Ericsson, M., Hiller, G., Machamer, C. E., Van 'T Hof, W., Van Meer, G., Moss, B., and Griffiths, G. (1993). Assembly of vaccinia virus: role of the intermediate compartment between the endoplasmic reticulum and the Golgi stacks. *J. Cell Biol.* 121, 521–541.

Stauber, R., Pfleiderera, M., and Siddell, S. (1993). Proteolytic cleavage of the murine coronavirus surface glycoprotein is not required for fusion activity. *J. Gen. Virol.* 74, 183–191.

Steegmaier, M., Levinovitz, A., Isenmann, S., Borges, E., Lenter, M., Kocher, H. P., Kleuser, B., and Vestweber, D. (1995). The E-selectin-ligand ESL-1 is a variant of a receptor for fibroblast growth factor. *Nature* 373, 615–620.

Stieber, A., Gonatas, J. O., Gonatas, N. K., and Louvard, D. (1987). The Golgi apparatus-complex of neurons and astrocytes studied with an anti-organelle antibody. *Brain Res.* 408, 13–21.

Stieber, A., Mourelatos, Z., Chen, Y-J, Le Douarin, N., and Gonatas, N. K. (1995). MG-160, A membrane protein of the Golgi apparatus which is homologous to a fibroblast growth factor receptor and to a ligand for E-Selectin, is found only in the Golgi apparatus and appears early in chicken embryo development. *Exp. Cell. Res.* 219, 562–570.

Swift, A. M., and Machamer, C. E. (1991). A Golgi retention signal in a membrane-spanning domain of coronavirus E1 protein. *J. Cell Biol.* 115, 19–30.

Taguchi, F. (1993). Fusion formation by the uncleaved spike protein of murine coronavirus JHMV variant cl-2. *J. Virol.* 67, 1195–1202.

Tooze, S. A., Tooze, J., and Warren, G. (1988). Site of addition of N-Acetyl-galactosamine to the E1 glycoprotein of mouse hepatitis virus-A59. *J. Cell Biol.* 1475–1487.

Turner, J. R., and Tartakoff, A. M. (1989). The response of the Golgi complex to microtubule alterations: The roles of metabolic energy and membrane traffic in Golgi complex organization. *J. Cell. Biol.* 109, 2081–2088.

Yoshida, T., Chen, C. C., Zhang, M. S., and Wu, H. C. (1991). Disruption of the Golgi apparatus by brefeldin A inhibits the cytotoxicity of ricin, modeccin, and Pseudomonas toxin. *Exp. Cell Res.* 192, 389–395.